HHS Public Access

Author manuscript

Clin Cancer Res. Author manuscript; available in PMC 2018 September 15.

Published in final edited form as:

Clin Cancer Res. 2017 September 15; 23(18): 5611–5621. doi:10.1158/1078-0432.CCR-16-3272.

Role of platelet-derived Tgfβ1 in the progression of ovarian cancer

Qianghua Hu[1], **Takeshi Hisamatsu**[2], **Monika Hammerle**[2], **Min Soon Cho**[1], **Sulina Pradeep**[2], **Rajesha Rupaimoole**[2], **Cristian Rodriguez-Aguayo**[3], **Gabriel Lopez-Berestein**[3], **Stephen T.C. Wong**[4], **Anil K. Sood**[2,5], and **Vahid Afshar-Kharghan**[1,5]

[1]Department of Benign Hematology, The University of Texas M. D. Anderson Cancer Center, Houston, TX 77030, USA

[2]Department of Gynecologic Oncology and Reproductive Medicine, The University of Texas M. D. Anderson Cancer Center, Houston, TX 77030, USA

[3]Department of Experimental Therapeutics, The University of Texas M. D. Anderson Cancer Center, Houston, TX 77030, USA

[4]Department of Systems Medicine and Bioengineering, Houston Methodist Research Institute, Weill Cornell Medicine, Houston, Texas 77030, USA

Abstract

Purpose—Transforming growth factor β1 (Tgfβ1) plays an important role in cancer. Most of Tgfβ1 in plasma is from platelets, thus we studied whether platelet Tgfβ1 has any role in the progression of ovarian cancer, and whether this role is limited to metastasis or also involves the growth of primary tumors.

Experimental Design—We compared the growth of murine ovarian cancer cell-induced tumors in platelet-specific Tgfβ1 deficient mice and wild-type mice. Using resected tumor nodules, we studied the effect of platelet Tgfβ1 on neoangiogenesis and on platelet extravasation into tumors. To investigate the effect of Tgfβ1 at different stages of ovarian cancer, we reduced expression of Tgfβ1 receptor (its TgfβR1 component) in tumors at different time points after injection of cancer cells, and compared the final tumor size.

Results—Lack of platelet Tgfβ1 in mice reduced tumor growth, neoangiogenesis, and platelet extravasation. Ovarian cancer tumors in platelet-specific Tgfβ1 deficient mice reached less than half of their size in wild-type littermates. Knockdown of TgfβR1on cancer cells in the first 2 weeks after their injection reduced tumor growth, but was less effective if initiated after 3 weeks.

[5]To whom correspondence should be addressed vakharghan@mdanderson.org and aksood@mdanderson.org.

The authors declare no potential conflicts of interest

Author contributions

QH designed and performed experiments and analyzed and interpreted data; TK, MH, MSC, SP, RP, and CR-A performed experiments and analyzed data; GL-B interpreted data; AKS designed experiments and interpreted data; and VA-K designed experiments, interpreted data, and wrote the manuscript.

Conflict-of-interest disclosure: The authors declare no competing financial interests.

Conclusions—We showed that platelet Tgfβ1 increased the growth of primary tumors in murine models of ovarian cancer. We also showed that inhibition of TgfβR1 is more effective in reducing the growth of ovarian cancer if initiated earlier. Our results supported a therapeutic benefit in preventing platelet activation, degranulation, and release of Tgfβ1 in ovarian cancer.

Keywords

platelets; cancer; cytokine; ovarian cancer; TGFβ1

Introduction

Platelets interact with cancer cells and play an important role in metastasis by inducing angiogenesis, promoting epithelial-mesenchymal transition (EMT), enhancing survival of circulating tumor cells (CTC), and facilitating extravasation of cancer cells to seed metastatic foci (1,2). Tgfβ1 secreted from activated platelets is involved in many steps of this process; Tgfβ1 enhances EMT in cancer cells through activation of Tgfβ/Smad and NF-kB pathways (3), and inhibits natural killer (NK) cells' antitumor activity by downregulating natural killer group 2 member D (NKG2D) on NK cells (4). We have shown that platelets, in addition to facilitating metastasis, also promote tumor growth in ovarian cancer by increasing proliferation of cancer cells (5). We demonstrated that the pro-proliferative effect of platelets on ovarian cancer cells is at least partially mediated by platelet-secreted Tgfβ1 (6). Blockade of Tgfβ1 by anti-Tgfβ1 antibodies or knockdown of Tgfβ1 receptor on ovarian cancer cells, reduced proliferation of ovarian cancer cells incubated with platelets *in vitro*. However, the *in vivo* effect of platelet-secreted Tgfβ1 on tumor growth is unknown. Platelets are the major source of Tgfβ1 in plasma and contain 40–100 times higher concentration of Tgfβ1 than other cells (7,8). In this study, we investigated the *in vivo* effect of Tgfβ1 originated from platelets on the growth of ovarian cancer by using conditional Tgfβ1 deficient mice that lack Tgfβ1 in platelets (3) in a murine model of orthotopic ovarian cancer (5,6,9). We compared the growth of tumors induced by injection of murine ovarian cancer cells into the peritoneum of mice with complete platelet-specific Tgfβ1 deficiency (*Tgfβ1*$^{fl/fl}$*;Pf4-Cre)*, mice with half-reduced platelet Tgfβ1 (*Tgfβ1*$^{fl/+}$*;Pf4-Cre)*, and wild-type control mice. Because of the role of Tgfβ1 in cell proliferation and angiogenesis (10–12), we also compared new blood vessel formation and proliferation of cancer cells in tumors resected from these mice.

There are two possible routes for platelet-secreted Tgfβ1 to reach cancer cells and tumor microenvironment (TME). First, platelets can directly interact with the endothelium of tumor microvasculature and release Tgfβ1 along with other proangiogenic factors (13) that subsequently reach TME through the fenestrated endothelium. Alternatively, platelets can extravasate into tumor microenvironment, where they become activated after interaction with cancer cells and with collagen in the extracellular matrix, and release a repertoire of growth factors including angiogenic factors (5,9,14). In this study, we investigated the effect of platelet Tgfβ1 on extravasation of platelets into TME.

We found that deficiency of platelet Tgfβ1 or blockade of TgfβR1 on tumor cells reduced the growth of the primary tumors, impaired neoangiogenesis, and reduced platelet extravasation into TME in murine models of ovarian cancer.

Material and Methods

All of the studies were conducted according to the protocols approved by the Institutional Review Board and Institutional Animal Care and Use Committee of the University of Texas MD Anderson Cancer Center.

Cell lines and culture conditions

All cell lines used in this study were obtained from the institutional Cell Line Core laboratory, authenticated every year per MD Anderson Cancer Center institutional policy ACA #1044, and routinely tested for mycoplasma contamination using the MycoAlert Kit (Lonza, Walkersville, USA). Human ovarian cancer cell line SKOV3ip1, which displays a higher degree of migration potential than its parental cell line SKOV3, was established from ascites from *Nu/Nu* mice given an intraperitoneal (i.p.) injection of SKOV3 cells. The SKOV3ip1 cells were cultured in RPMI-1640 supplemented with 10% to 15% FBS and 0.1% gentamicin sulfate; murine ovarian cancer cell lines IG10 and ID8 (15) were grown in DMEM medium supplemented with 5% FBS, 0.1% gentamicin sulfate, and 1% Insulin-Transferrin-Sodium Selenite (Roche, Indianapolis, USA). Cells were maintained at 37°C in a humidified incubator infused with 20% O_2 and 5% CO_2.

Mice and murine model of ovarian cancer

Female athymic nude (NU/NU) mice and syngeneic C57BL/6 WT mice were purchased from the Department of Veterinary Medicine and Surgery, M D Anderson Cancer Center. Platelet-specific Tgfβ1-deficient (complete knockout) mice (*Tgfβ1*$^{fl/fl}$;*Pf4-Cre* or briefly *pTgfβ1*$^{-l-}$) were a gift from Richard O. Hynes (MIT, Cambridge, MA, USA) (3). Platelet-specific Tgfβ1 half knockout mice (*Tgfβ1*$^{fl/+}$;*Pf4-Cre* or briefly *pTgfβ1*$^{+l-}$) were generated by crossing C57BL/6 WT with *pTgfβ1*$^{-l-}$ mice. Genotyping was carried out following the previously described protocol (3). Orthotopic murine models of ovarian cancer were generated by intraperitoneal (i.p.) injection of cancer cells to 8–10 weeks old females (16). In the syngeneic model, 1×10^6 IG10 or ID8 murine ovarian cancer cells were resuspended in 200 μl of Hank's balanced salt solution and injected into the peritoneum of the mice consisting of 3 genotypes, *i.e.*, C57BL/6 WT, *pTgfβ1*$^{+l-}$, and *pTgfβ1*$^{-l-}$. Mice maintained for 8–10 weeks after injection became moribund and were sacrificed. In the athymic nude model, the same number of human ovarian cancer cells (SKOV3ip1) were injected intraperitoneally to *NU/NU* mice. In this model, mice were treated every 3 days (starting at different time points as shown in Figure 3) for different durations with either scrambled siRNA or human (h)TgfβR1 siRNA. About 6 weeks after injection of cancer cells, mice became moribund and were sacrificed. Tumor nodules were resected from the peritoneum, counted, and weighed. Some tumor nodules were fixed in formalin, and others were saved as fresh frozen samples by embedding in optimum cutting temperature (O.C.T.) compound.

siRNA transfection and in vivo delivery

Predesigned or customized human -specific small interfering RNAs (siRNAs), and scrambled siRNA were purchased from Sigma-Aldrich (The Woodlands, USA). Three hTgfβR1 siRNAs reduced TgfβR1 mRNA level in SKOV3ip1 cells *in vitro*. The sequences of siRNAs were 5′-GGUCAAUUGUUCUACCUCATT-3′ (sense), 5′-UGAGGUAGAACAAUUGACCTT-3′ (anti-sense); 5′-CUGUGAAGCCUUGAGAGUATT-3′ (sense), 5′-UACUCUCAAGGCUUCACAGTT-3′ (anti-sense); and 5′-GGGUCUGUGACUACAACAUTT-3′ (sense) and 5′-AUGUUGUAGUCACAGACCCTT-3′ (anti-sense). We used the most efficient TgfβR1 siRNA (underlined) for *in vivo* delivery to the tumor-bearing mice. For *in vitro* transfections, 2μl of 75.2 μM or a total of 2 μg TgfβR1 siRNA and 3 μl Lipofectamine (Thermo Fisher, Carlsbad, USA) were each first diluted in 100 μl of serum free media, then mixed and incubated for 30 min. The mixture was added to 5×10^5 cells in a six-well plate in serum-free media (1 ml) and incubated for 6 h. The final concentration of the siRNA was 125.3 nM. Transfected cells were maintained for 2 d in complete media. For *in vivo* delivery, siRNAs were incorporated into DOPC-based liposomes. Briefly, siRNAs were mixed with DOPC in the p11.3resence of excess tertiary butanol (1:10 w/w siRNA/DOPC), then mixed with Tween 20 (1:19 v/v Tween 20/siRNA-DOPC), and finally lyophilized and stored at −80°C until use. Immediately prior to i.p. injection, the lyophilized preparation was hydrated with 0.9% saline (16). In each injection, 11.3 nmol (150 μg)/kg/mouse TgfβR1 siRNA was administered.

Mouse platelet isolation

Mice were anesthetized and laparotomy was performed. Whole blood was drawn from the inferior vena cava into a 1 ml syringe preloaded with 130 μl of 3.8% sodium citrate, and mixed 1:1 (vol/vol) with Tyrodes buffer lacking Mg^{2+} and Ca^{2+}. Blood was centrifuged at 1,100 rpm (200 × *g*) for 6 minutes at room temperature. At the same time, Sepharose 2B beads (Sigma-Aldrich, St. Louis, USA) were prepared by washing once in an equal volume of acetone and twice in an equal volume of cold PBS. The platelet-rich plasma fraction was passed through a filtration column of Sepharose 2B beads loaded into a siliconized glass column with a 10-μm nylon net filter (Millipore, Billerica, USA). Cloudy eluents, which contained platelets, were collected. Platelets were counted with a hemocytometer by phase-contrast microscope at ×400 magnification and immediately used for subsequent experiments (9).

Intravital fixation

Mice were anesthetized with isoflurane, and an incision was made in the chest cavity to expose the left heart. A 21-gauge needle in connection with a solution-filled syringe was then used to slowly deliver PBS and 4% paraformaldehyde (9).

Western blot analysis

Cultured cells were washed with cold phosphate buffered saline (PBS) and lysed in a buffer consisting of 1% Triton X-100, 50mM HEPES, pH 7.4, 150mM NaCl, 1.5mM $MgCl_2$, 1mM EGTA, 100mM NaF, 10mM Na pyrophosphate, 1mM Na_3VO_4, 10% glycerol, and freshly

added protease and phosphatase inhibitors from Roche Applied Science (Indianapolis, USA). Protein concentrations of the lysates were determined by a BCA Protein Reagent Kit (Pierce Biotech., Rockford, USA), and 25 μg of proteins were subjected to gel electrophoresis on 10% SDS-PAGE gels. Antibodies used were against TgfβR1 (Santa Cruz, Dallas, USA, sc-398, at 1:200 dilution), and β-ACTIN (Sigma-Aldrich, St. Louis, USA, A5316, 1:5000) (17).

Quantitative real-time PCR

Total RNA was isolated from ovarian cancer cell lines (SKOV3ip1, ID8) using mirVana miRNA Isolation Kit (ThermoFisher Scientific, Austin, USA). Following a previously described method (18), mRNA level was quantified by one-step SYBR Green assays (2 assays and triplicate per each sample) using the Vii™ 7 Rea-Time PCR System (Applied Biosystem of ThermoFisher Scientific, Foster City, USA) The following RT-PCR primers were used: TgfβR1 (human), 5′-TGG CTC AGG TTT ACC ATT GC-3′ (forward), and 5′-TTC TCC AAA TCG ACC TTT GC-3′ (reverse); TgfβR1 (mouse), 5′-TGC CAT AAC CGC ACT GTC A-3′ (forward), and 5′-AAT GAA AGG GCG ATC TAG TGA TG-3′ (reverse); GAPDH (human), 5′-GGT CTC CTC TGA CTT CAA CA-3′ (forward), and 5′-GTG AGG GTC TCT CTC TTC CT-3′ (reverse); Gapdh (mouse), 5′-CGA CTT CAA CAG CAA CTC CCA CTC TTC C-3′ (forward), and 5′-TGG GTG GTC CAG GGT TTC TTA CTC CTT-3′ (reverse).

Cell proliferation analysis

Fifty thousand cells IG10 or ID8 were plated in 6-well plates and grown in serum-free media (SFM) for 24 h. Mouse platelets (20×10^6 per well) isolated as described above were added to the cells. After 48 h of incubation, cell proliferation was analyzed using the BrdU labeling and Detection Kit (Roche, Indianapolis, USA) according to the manufacturer's instructions. Briefly, cells were pulse-labeled with 10 μM BrdU for 90 min, washed three times with PBS, detached with 0.25% Trypsin-EDTA, fixed with 70% ethanol fixative for 20 min, immunostained with mouse anti-BrdU primary antibody and anti-mouse Ig-fluorescein secondary antibody, and finally analyzed using flow cytometry (EPICS XL 4-Color Cytometer; Beckman Coulter, Brea, USA). The assay was performed for 3 times.

Immunohistochemical staining

Immunohistochemical analysis on Ki67 for tumor proliferation assessment was carried out using a Vectastain ABC (avidin-biotin-peroxidase) kit (Vector Laboratories, Burlingame, USA) as recommended by the manufacturer. Briefly, 5-μm formalin-fixed and paraffin-embedded tumor sections were deparaffinized with xylene and decreasing concentrations of ethanol and rehydrated with PBS. Antigen retrieval was performed using 1× Borg-decloaker (BioCare Medical, Pacheco, USA) under steamer cooker at 65°C for 45 min followed by natural cool-down to room temperature. Endogenous peroxidases were blocked with 3% hydrogen peroxide in PBS. Nonspecific binding was blocked with 5% normal horse serum and 1% normal goat serum in PBS for 30 min. Primary anti-Ki67 polyclonal antibody (Abcam, ab15580, 1:200) (Cambridge, USA) was incubated for 1 h. After being washed three times with PBS, the sections were incubated with the biotinylated secondary antibody (Vector Laboratories, Burlingame, USA) for 45 min at room temperature. After incubation

with the avidin-biotin-peroxidase complex for 45 min, the sections were washed with PBS. The color was developed with 3,3′-diaminobenzidine (DAB) substrate. The sections were dehydrated and mounted with Permount (Fisher Scientific, Pittsburg, USA) and examined with a Leica DMR epifluorescence microscope, and images were captured by a Hamamatsu C5810 charge-coupled device camera. To quantify Ki67 positivity, from each group 5 mice, and from each mouse 3 tumor nodules, and from each tumor nodule 2 sections were studied. In each section, 6 random fields (200 X magnification) were examined. In each field the number of Ki67 positive cells was divided by the total number of cells and multiplied by 100 to obtain the %Ki67 positivity in that field. The average %Ki67 positivity of all examined fields in each group of mice was calculated and used for comparisons between different groups.

Co-immunofluorescence analyses for measurement of blood vessel density and quantification of extravascular platelets

Co-immunofluorescence analyses for CD42b1 and CD31 were performed on 5-μm O.C.T. compound-embedded fresh frozen tumor sections. Slides were fixed and permeabilized with acetone and acetone:chloroform and rehydrated with PBS. Nonspecific binding was blocked with 5% normal donkey serum (DS) and 1% BSA in PBS for 20 min. Primary goat anti-CD42b1 (Santa Cruz) and rat anti-CD31 (BD Pharmingen, San Diego, USA) were diluted in 2.5% DS and 1% BSA by 1:100 and 1:400, respectively. The antibodies were sequentially incubated for 1 h each at room temperature. After washing with PBS × 3 times, each wash for 5 min, appropriate fluorescence-labeled secondary antibodies (ThermoFisher Scientific, Eugene, USA) along with 4′,6-diamidino-2-phenylindole (DAPI) were incubated for 1 h in dark at room temperature. After 3 washes with PBS, a ProLong antifade reagent (ThermoFisher Scientific) was used to complete the mounting of the coverslip. Images were then acquired with a Leica DMR epifluorescent microscope and the Metamorph software program (Universal Imaging). To assess the density of mature blood vessels, a previously described method which takes into account the heterogeneity of tumor blood vessels was followed (16,17). Stained slides were scanned at low power (×40) to locate areas of highest vascularity. Over 10 high powered (×200) fields within these areas were randomly selected and mature blood vessel densities were determined by counting CD31-positive structures which displayed lumen or tubular anatomy. Similarly, to quantify extravascular platelets, areas with impressive platelets staining and high vascularity were first located at low power scanning (×40) and over 20 high powered (×400) fields were randomly selected within these areas. The number of extravasated platelets was determined by counting them in the selected fields.

Statistics

Statistical analysis was performed using Microsoft Excel. One-way ANOVA analysis was performed to compare a variable across ≥ 3 groups. F-test with $p < 0.05$ was considered to be significant. Comparisons between two groups were made using the Student's t-test with $p < 0.05$ being considered statistically significant. All data for measured variables were expressed as means ± SEM. All of ANOVA analyses showed a $p < 0.005$. The F-test and t-test results were reported as indicated.

Results

Platelet-secreted Tgfβ1 promotes tumor growth

To determine the *in vivo* role of platelet-specific Tgfβ1 on tumor growth, we used mice with 3 genotypes (*WT*, $pTgf\beta1^{+l-}$, *and* $pTgf\beta1^{-l-}$) in syngeneic orthotopic ovarian cancer models induced by the intraperitoneal injection of murine ovarian cancer cells (IG10 and ID8). Aggregate tumor weight induced by IG10 cells in mice with complete *Tgfβ1* deficiency ($pTgf\beta1^{-l-}$) was reduced by 63% as compared to that in WT mice (0.18 ± 0.04 g *vs* 0.48 ± 0.06 g, respectively, $p < 0.001$, n = 10) (Figure 1A). Growth of tumors induced by ID8 cells in $pTgf\beta1^{-l-}$ mice was 47% less than that in WT mice (0.49 ± 0.11 g *vs* 0.93 ± 0.10 g, $p < 0.05$, n = 10) (Figure 1B). Partial Tgfβ1 deficiency in platelet of $pTgf\beta1^{+l-}$ mice, with a plasma Tgfβ1 level at 44% of that in WT mice (3), resulted in a significant reduction (35% for IG10 and 43% for ID8, respectively) in tumor weight compared to WT mice for both cell lines (0.31 ± 0.04 g *vs* 0.48 ± 0.06 g, $p < 0.05$ for IG10; 0.53 ± 0.09 g *vs* 0.93 ± 0.10 g, $p < 0.005$ for ID8) (Figure 1A–B). While the effect of a partial platelet Tgfβ1 deficiency in ID8-induced tumors was to the same magnitude as that of its complete deficiency (0.53 ± 0.09 g in $pTgf\beta1^{+l-}$ mice *vs* 0.49 ± 0.11 g in $pTgf\beta1^{-l-}$ mice, $p = 0.82$), there was a gene-dose effect regarding Tgfβ1 deficiency and growth of IG10-induced tumors; with tumors in mice reaching an intermediate size between their size in WT and $pTgf\beta1^{-l-}$ mice. The number of tumor nodules, another measure of tumor growth and aggressiveness, in $pTgf\beta1^{-l-}$ mice was also significantly reduced by about 2/3 in comparison to WT mice for both cell lines (Figure S1).

We measured the proliferation rate of cancer cells in resected tumor nodules using Ki67 immunostaining. In IG10-induced tumors, the percentage of Ki67 positivity in $pTgf\beta1^{-l-}$ mice was 46% less than WT mice (21.4% ± 1.96% *vs* 39.6% ± 2.2%, respectively, $p < 0.001$). The Ki67 positivity in IG-10-induced tumors in $pTgf\beta1^{+l-}$ mice (30.3% ± 1.96%) was 23% less than WT mice ($p = 0.009$) and 41% more than $pTgf\beta1^{-l-}$ mice ($p = 0.007$) (Figures 1C & 1E). In ID8-induced tumors, the corresponding reduction in Ki67 in $pTgf\beta1^{-l-}$ mice compared to WT mice was 37% (41.4% ± 3.18% *vs* 65.8% ± 3.16%, $p < 0.001$). The Ki67 positivity in ID8-induced tumors in $pTgf\beta1^{+l-}$ mice (43.1% ± 3.36%) was 34% less than WT mice ($p < 0.001$) but was not significantly different than $pTgf\beta1^{-l-}$ mice ($p = 0.71$) (Figures 1D & 1F).

We assessed the effect of platelet Tgfβ1 on the amount of ascites induced by IG10 and ID8 tumors. For IG10-induced tumors, the amount of ascites in $pTgf\beta1^{-l-}$ mice was 71% less than WT mice (0.83 ± 0.08 ml *vs* 2.85 ± 0.27 ml, $p < 0.001$). The amount of ascites in $pTgf\beta1^{+l-}$ mice (2.05 ± 0.25 ml) was 28% less than WT mice ($p = 0.05$) but 2.5 folds higher than $pTgf\beta1^{-l-}$ mice ($p < 0.001$). For ID8 tumors, the amount of ascites in $pTgf\beta1^{-l-}$ mice was 63% less than WT mice (2.83 ± 0.75 ml *vs* 7.69 ± 1.11 ml, $p = 0.002$). The amount of ascites in $pTgf\beta1^{+l-}$ mice (3.14 ± 0.76 ml) was 59% less than WT mice ($p = 0.004$) and was not significantly different than $pTgf\beta1^{-l-}$ mice ($p = 0.77$). These data suggested that the effect of platelet Tgfβ1 on the amount of ascites followed a similar pattern to its effect on the growth of orthotopic tumors. A comparison between the two murine ovarian cancer cell

lines showed that ID8 cells generated 2.7 times more ascites than IG10 cells in WT mice (7.69 ± 1.11 ml *vs* 2.85 ± 0.27 ml, $p = 0.002$).

Platelet-secreted Tgfβ1 stimulates cancer cell proliferation in vitro

We investigated the *in vitro* effect of platelet Tgfβ1 on cell proliferation by incubating cancer cells with platelets isolated from mice with different genotypes ($pTgfβ1^{-|-}$, $pTgfβ1^{+|-}$, and WT). When WT platelets were co-cultured with murine ovarian cancer cells in serum free media (SFM) for 24 h, cell proliferation, as quantified by BrdU incorporation, increased by more than 4 folds in IG10 cells (no platelets: 6.17% ± 0.5% vs WT platelets: 25.48% ± 1.91%, p <0.001) (Figure 2A) and ~3.5-fold for ID8 (no platelets: 9.71% ± 0.91% vs WT platelets: 32.39% ± 1.71%, p <0.001) (Figure 2B). Compared to wild-type platelets, complete Tgfβ1 deficiency reduced proliferation rate in IG10 by 73% and in ID8 cells by 65%, respectively (Figure 2A–B). Partial Tgfβ1 deficiency in platelets resulted in reduction of platelet-enhanced cell proliferation by 27% in IG10 cells (WT 25.48% ± 1.91% vs half KO 18.66% ± 1.66%, $p <0.05$) and 30% in ID8 (WT 32.39% ± 1.71% vs half KO 22.75% ± 1.58%, $p <0.05$). Complete deficiency of Tgfβ1 in platelets resulted in an additional 39% reduction in cell proliferation in IG10 cells (11.35% ± 1.06%) and ~23% reduction in ID8 cells (17.58% ± 1.18%) compared to that achieved by partial Tgfβ1 deficiency (both statistically significant). These data showed a pro-proliferative effect of platelet-derived Tgfβ1 on IG10 and ID8 cells, and are consistent with our previous observation that TgfβR1 knockdown on ID8 murine ovarian cancer cells reduced platelet-enhanced proliferation in ID8 cells (6).

Reducing TgfβR1 expression on ovarian cancer cells reduced tumor growth in vivo in a time-dependent manner

To dissect the early versus late effects of Tgfβ1 on the growth of ovarian cancer, we reduced expression of Tgfβ1 receptor on ovarian cancer cells at different time points after injection to mice. We used siRNA targeting TgfβR1, the signaling component of Tgfβ1 receptor, to reduce expression and signaling of TgfβR1 on a human ovarian cancer cell line (SKOV3ip1). We used human TgfβR1 siRNAs, and identified 3 siRNAs that reduced TgfβR1 mRNA in SKOV3ip1 by more than 75%, as compared to scrambled control siRNA. Transfection of the most efficient siRNAs reduced TgfβR1 mRNA by 83% and TgfβR1 protein by 90% in SKOV3ip1, respectively (Figure 3A–B), but did not affect the expression of TgfβR1 mRNA in murine ovarian cancer cell lines, IG10 and ID8 (Figure S2).

Two days after i.p. injection of SKOV3ip1 cells, mice were divided into 6 groups (n=10/group). In the first group (control), mice received scrambled siRNA by i.p. injections every 3 days for a total of 15 injections (a total of 46 days after implanting cancer cells). In the other 5 experimental groups, mice received i.p. injections of human (h)TgfβR1 siRNA every 3 days starting at days 2 (G1), 8 (G2), 14 (G3), 20 (G4), and 26 (G5) post tumor cell injection, respectively (Figure 3C). Compared to the control group, injection of hTgfβR1 siRNA within 2 weeks after injection of SKOV3 significantly reduced average aggregate tumor weights: 1.22 ± 0.12 g for the control group vs 0.52 ± 0.07 g (G1), 0.63 ± 0.11 g (G2), 0.63 ± 0.09 g (G3); corresponding to 57% ($p < 0.001$), 48% ($p < 0.005$), and 48% ($p < 0.005$) reduction in tumor weight in the experimental groups G1–3, respectively. Injection of

hTgfβRI siRNA starting after day 20 in the experimental groups G4 and G5, did not change the final tumor size significantly compared to the control group (Figure 3D). In contrast, the number of tumor nodules reduced significantly in all 5 experimental groups (Figure S1). Cancer cell proliferation rate assessed by the percentage of Ki67 positivity was significantly reduced in experimental groups G1–G3, as is shown in the comparison between tumors resected from the control group and the experimental group G1 that received the longest administration of hTgfβR1 siRNA. The Ki67 positivity was 69.6% ± 3.6% in the control group and 37.7% ± 2.3% in the G1 group ($p < 0.001$) (Figure 3E & F). There was no significant difference between G1, G2, and G3 regarding Ki67 positivity (data not shown). To confirm the *in vivo* effectiveness of hTgfβR1 siRNA, tumor nodules resected from hTgfβR1 siRNA- or scrambled siRNA-treated tumor-bearing mice were examined for expression of TgfβR1. Both TgfβR1 protein (Figure 3E) and mRNA (Figure 3G) was drastically reduced in tumor nodules resected from mice treated with hTgfβR1 siRNA. Furthermore, phosphorylated SMAD2 (a signaling protein downstream to TgfβR1), was also significantly reduced (Figure 3E). hTgfβR1 siRNA reduced the relative hTgfβR1 mRNA level by 61% (from 100.0 ± 5.5 in scrambled siRNA nodules to 39.1 ± 4.3 in hTgfβR1 siRNA nodules, $p < 0.001$) (Figure 3G).

Role of platelet-secreted Tgfβ1 in tumor angiogenesis and platelet extravasation into TME

We investigated the number and organization of CD31+ endothelial cells in tumor nodules resected from tumor-bearing mice with different genotypes (*WT*, *pTgfβ1*$^{+|-}$, *and* *pTgfβ1*$^{-|-}$). Immunofluorescence (IF) staining showed that the overall number of CD31^{+} endothelial cells are not significantly different in ID8- or IG10-induced tumor nodules between WT and Tgfβ1 deficient mice. We had a similar observation in tumors induced by human ovarian cancer cells (SKOV3ip1) in nude mice treated with scrambled siRNA or hTgfβR1 siRNA. However, in both murine and human ovarian cancer cell-induced tumors, platelet Tgfβ1 deficiency reduced the number of mature blood vessels, as determined by the number of lumens encircled by CD31+ cells. To quantify the density of blood vessels, we examined tumor nodules from 5 mice in each group, at least 3 nodules per mouse, one section per nodule, and 2 or more high-power fields (HPF) per section by IF microscopy. In IG10 and ID8-induced tumors, complete platelet Tgfβ1 deficiency reduced the density of mature blood vessels by 35% and 45% compared to tumor nodules in WT mice, respectively (for IG10, WT: 8.40 ± 0.88 *vs* Tgfβ1 KO: 5.47 ± 0.66, $p < 0.05$; for ID8, WT: 9.90 ± 0.77 *vs* Tgfβ1 KO: 5.41 ± 0.80, $p < 0.001$). In SKOV3ip1-induced tumors in *Nu/Nu* mice, knockdown of TgfβR1 resulted in 71% reduction in the density of mature blood vessels (scrambled siRNA: 5.90 ± 0.62 *vs* hTgfβR1 siRNA: 1.70 ± 0.30, $p < 0.001$) (Figure 4A).

To determine the number of extravasated platelets, tumor sections were immunostained for CD31 and CD42b, and examined with fluorescence microscopy to identify intratumor and extravascular platelets (CD42b+). We examined tumor nodules from 5 mice/group, ≥3 nodule/mouse, 2 sections/nodule, and ≥2 HPF/section. In SKOV3ip1-induced tumor nodules, hTgfβR1 siRNA reduced the number of extravasated platelets by 51% as compared to scrambled control siRNA (scrambled siRNA 7.95 ± 1.12 *vs* hTgfβR1 siRNA 3.86 ± 0.53, $p < 0.005$) (Figure 4B). Number of extravasated platelets in IG10- and ID8-induced tumors in platelet-specific Tgfβ1 deficient mice decreased by 27% and 30%, respectively, compared

to WT mice; although the magnitude of reduction was not statistically significant (for IG10, WT: 5.83 ± 0.85 *vs* *pTgfβ1*$^{-/-}$: 4.27 ± 0.77, $p = 0.35$; for ID8, WT: 6.05 ± 0.86 *vs* *pTgfβ1*$^{-/-}$: 4.23 ± 0.67, $p = 0.21$) (Figure 4A).

Putting together, these results showed that platelet-derived Tgfβ1 is important for neoangiogenesis in tumors. Our data also supported a possible role for Tgfβ1 signaling in ovarian cancer cells, induced by sources other than platelets in TME, in promoting platelet extravasation into the tumor.

Discussion

In this study, we investigated the effect of platelet Tgfβ1 on the growth of ovarian cancer. Role of platelets in metastasis (19) and role of Tgfβ1 in tumorigenesis (20) and progression of cancer (21) have been studied extensively. In an elegant study, Labelle et al. have shown that the prometastatic effect of platelets is partially mediated by platelet Tgfβ1 activating Smad signaling pathway in cancer cells (3). We have previously shown that platelets not only promote metastasis but also enhance the growth of primary tumors in ovarian cancer by increasing proliferation of cancer cells (5,6). We showed that the direct effect of platelets on the proliferation rate of ovarian cancer cells can be reduced by Tgfβ1 blocking antibodies or by reducing the expression of TgfβR1 on ovarian cancer cells *in vitro*. In the current study, we evaluated the effect of platelet-derived Tgfβ1 on proliferation of cancer cells, by incubating platelets isolated from a conditional knockout mice deficient in platelet Tgfβ1 with ovarian murine ovarian cancer cells (IG10 and ID8). Our data suggested that platelets directly increase cancer cell proliferation in a Tgfβ1 dose-dependent manner. Besides Tgfβ1 other platelet factors also contribute to cancer cell proliferation, because even platelets completely deficient in Tgfβ1 increased cancer cell proliferation by 30% ($p < 0.005$) (Figure 2). We showed a role for platelet's Tgfβ1 and cancer cell's TgfβR1 in the growth of primary tumors in murine models of ovarian cancer, using platelet-specific Tgfβ1 knockout mice and siRNA-mediated reduction in TgfβR1 on ovarian cancer cells. We found that lack of Tgfβ1 in platelets or lack of TgfβR1 on ovarian cancer cells reduced the growth of orthotopic ovarian cancer in mice by 50%. Although platelets are the major source of Tgfβ1 in serum and mice deficient in platelet Tgfβ1 have 90% reduction in Tgfβ1 concentration in serum (3), cancer cells and several other cellular components of tumor microenvironment (endothelial cells, fibroblasts, macrophages) also secrete Tgfβ1 (22) and contribute to the local concentration of Tgfβ1 inside tumors. However, we found that lack of Tgfβ1 originated from platelets reduced tumor growth to the same magnitude as lack of TgfβR1 on cancer cells, and this might be interpreted as platelets being the main source of Tgfβ1 inside ovarian cancer tumors. We investigated the effect of platelet Tgfβ1 on angiogenesis and platelet extravasation into the tumor. Our data indicated that platelet Tgfβ1 is important for neoangiogenesis inside orthotopic tumors in murine models of ovarian cancer. This observation is consistent with a recent study reporting a reduction in endothelial cells tube formation after inhibition of Tgfβ1 receptor signaling in an *in vitro* assay (23). Tgfβ1 regulates tumor angiogenesis by upregulating expression and activity of two potent proangiogenic factors, vascular endothelial growth factor (VEGF) and basic fibroblast growth factor (bFGF) (24–26). The effect of bFGF on angiogenesis itself is partially mediated through VEGF. Reduced angiogenesis in orthotopic tumors of mice in the absence

of platelet Tgfβ1 or in the absence of TgfβR1 on cancer cells might largely be due to a downregulation of VEGF inside tumors, as was shown in a study reporting a reduction in VEGF in SKOV3ip1-induced tumors in nude mice treated with systemic Tgfβ1 signaling inhibitor (27). Due to the large number of mice required for *in vivo* TgfβR1 knockdown experiments, we used only SKOV3ip ovarian cancer cell line in these experiments, but we also showed the pro-proliferative effect of platelet Tgfβ1 on high-grade serous ovarian cancer cell lines (OVCAR432 and CaOV3) *in vitro* (Figure S3). It is also important to mention that our *in vivo* studies on the effect of hTgfβR1 siRNA was based on examining the growth of human cancer cells in mice and thus was based on the interaction between mouse Tgfβ and human TgfβR1.

In our studies, reduction of TgfβR1 on ovarian cancer cells affected platelet extravasation more than lack of Tgfβ1 in platelets. Administration of hTgfβ1 siRNA reduced the number of platelets in orthotopic tumors induced by human ovarian cancer cells in nude mice by 51% ($p<0.005$). Reduction in the number of extravasated platelets in tumors induced by murine ovarian cancer cells in mice deficient in platelet Tgfβ1 did not reach a statistical significance (30% reduction, $p=0.25$). This points to the possibility that Tgfβ1 in TME originated from sources other than platelets such as cancer cells, endothelial cells, fibroblasts, infiltrating or resident white blood cells (22,25) is important for platelet extravasation.

Effect of Tgfβ1 in development and progression of cancer differs in the early phases of tumorigenesis and later in tumor progression and expnasion. Tgfβ1 inhibits proliferation and malignant transformation of benign epithelial cells, including ovarian surface epithelium (28). However, after tumor development, Tgfβ1 promotes tumor progression (28,29). Several drugs targeting Tgfβ protein superfamily, Tgfβ receptors, or Tgfβ signaling pathway (mostly small molecules inhibiting the kinase activity of TgfβR1) have been used in preclinical and clinical studies (20). Tgfβ receptors are oligomeric complexes formed by TgfβR1 and TgfβR2. TgfβR3 acts as a Tgfβ protein superfamily co-receptor (30). Progesterone decreases expression of TgfβR1 and increases TgfβR2/R3 on normal epithelial cells and that might explain the protective effect of progesterone against ovarian cancer (31). TgfβR3 suppresses ovarian tumorigenesis and its expression is reduced or lost on malignant ovarian epithelium (32). Tgfβ ligand proteins bind to TgfβR2 that activates TgfβR1. TgfβR1, in turn, interacts with Smad proteins and propagates intracellular signaling. We studied the effect of TgfβR1 signaling on the progression of cancer by reducing expression of TgfβR1 on ovarian cancer cells in a murine model of ovarian cancer. In order to compare the effect of earlier versus later inhibition of Tgfβ signaling, we injected tumor-bearing mice with TgfβR1 siRNA at different time intervals after injection of cancer cells. To differentiate the effect of Tgfβ1 on ovarian cancer cells from its effect on the other components of the tumor microenvironment, we used human-specific TgfβR1 siRNA to reduce expression of TgfβR1 only on SKOV3ip human ovarian cancer cells injected into nude mice. Earlier initiation of hTgfβR1 siRNA therapy (i.e. during the first 2 weeks after injection of cancer cells) reduced the growth of tumors significantly, but the initiation of therapy after 3 weeks did not significantly affect tumor growth. Because injected ovarian cancer cells were already malignant, these results would not alleviate the concerns about a possible risk for promoting tumorigenesis by inhibiting Tgfβ signaling, but showed a possible therapeutic benefit of

inhibiting Tgfβ1 signaling from the earliest stage of tumor progression. However, this would limit the use of Tgfβ inhibitors because many ovarian cancer patients are diagnosed in the later stages of their disease. Our data also raises the possibility of a therapeutic benefit for using anti-platelet reagents in early stages of ovarian cancer to prevent release of Tgfβ from platelets.

The effect of Tgfβ1 on tumor growth has been attributed to its effect on different cellular components of the tumor (cancer cells, fibroblast, endothelial cells, and leukocytes). We investigated whether the effect of platelet Tgfβ1 has any direct effect on ovarian cancer cells, by incubating murine ovarian cells with platelets from *pTgfβ1*$^{+|-}$, *or pTgfβ1*$^{-|-}$ mice *in vitro*. We found that Tgfβ1 from platelets directly increases proliferation in ovarian cancer in a gene dose-dependent manner. However, even Tgfβ1 deficient platelets increased proliferation rate in ovarian cancer cells compared to buffer, showing that other platelet factors besides Tgfβ1 also contribute to the pro-proliferative effect of platelets. In summary, our study provides the first evidence supporting an *in vivo* pro-growth effect of platelet-derived Tgfβ1 on primary tumors in ovarian cancer, mediated by increasing cancer cell proliferation. Platelet Tgfβ1 promoted neoangiogenesis in tumors by regulating the formation of mature blood vessels. Platelet extravasation into ovarian cancer tumors was partly regulated by the effect of Tgfβ1 on cancer cells. Inhibition of Tgfβ1 signaling if initiated early during the course of tumor progression reduced tumor growth *in vivo*.

Tgfβ inhibitors that trap Tgfβ (ligand), block Tgfβ receptors, or inhibit TgfβR kinase activity have been used in pre-clinical and clinical trials (20,24,33,34). These trials have provided information about the side effects of Tgfβ inhibitors, including detected side effects, and expected but non-detected side effects. Tgfβ is an important regulator of immune tolerance and inhibition of Tgfβ was expected to cause autoimmune disorders and inflammation, which were not detected in patients and mice treated with Tgfβ inhibitors. Due to a dual role of Tgfβ in cancer, acting as a tumor suppressor in the early stages of tumorigenesis and as a pro-growth and pro-metastatic factor in the later stages of tumorigenesis, a main concern was that inhibiting Tgfβ pathway would result in progression of premalignant lesions to cancer (34,35). In a clinical trial using a humanized anti-pan-Tgfβ monoclonal antibody in patients with malignant melanoma, dose-related skin lesions including non-malignant keratoacanthomas and squamous cell carcinoma on sun damaged skin were reported, but subsequent evaluation of the non-melanoma lesions were interpreted to be mostly non-malignant, which often resolved or improved after discontinuation of treatment (33). Another important finding in the preclinical trials was that the long-term use of a TgfβR kinase inhibitor in murine models of skin cancer resulted in an acquired resistance to this reagent (36). Intermittent and short term use of Tgfβ inhibitors in combination with cytotoxic reagents or radiotherapy can be a rational design for utilizing these reagents. One possible interpretation of our data is that inhibiting platelets, as a main source of Tgfβ for ovarian cancer cells, by anti-platelet reagents can also be used as a therapeutic approach circumventing side effects associated with Tgfβ inhibitors. Preventing platelet activation reduces platelet degranulation and release of Tgfβ1 in ovarian cancer. However, our data in murine models of ovarian cancer need to be confirmed by additional studies in the future in models closer to the human high-grade serous ovarian cancer that is the most common type of ovarian cancer in women.

Supplementary Material

Refer to Web version on PubMed Central for supplementary material.

Acknowledgments

Grant Support

This work was supported in part by R01CA177909 (to V.A-K. and A.K.S.), Ovarian Cancer Research Fund (Grant number 258813 to V.A-K. and A.K.S).

References

1. Labelle M, Hynes RO. The initial hours of metastasis: the importance of cooperative host-tumor cell interactions during hematogenous dissemination. Cancer discovery. 2012; 2(12):1091–9. DOI: 10.1158/2159-8290.cd-12-0329 [PubMed: 23166151]
2. Leblanc R, Peyruchaud O. Metastasis: new functional implications of platelets and megakaryocytes. Blood. 2016; 128(1):24–31. DOI: 10.1182/blood-2016-01-636399 [PubMed: 27154188]
3. Labelle M, Begum S, Hynes RO. Direct signaling between platelets and cancer cells induces an epithelial-mesenchymal-like transition and promotes metastasis. Cancer Cell. 2011; 20(5):576–90. [PubMed: 22094253]
4. Kopp HG, Placke T, Salih HR. Platelet-derived transforming growth factor-beta down-regulates NKG2D thereby inhibiting natural killer cell antitumor reactivity. Cancer Res. 2009; 69(19):7775–83. [PubMed: 19738039]
5. Stone RL, Nick AM, McNeish IA, Balkwill F, Han HD, Bottsford-Miller J, et al. Paraneoplastic thrombocytosis in ovarian cancer. NEnglJMed. 2012; 366(7):610–8.
6. Cho MS, Bottsford-Miller J, Vasquez HG, Stone R, Zand B, Kroll MH, et al. Platelets increase the proliferation of ovarian cancer cells. Blood. 2012; 120(24):4869–72. [PubMed: 22966171]
7. Meyer A, Wang W, Qu J, Croft L, Degen JL, Coller BS, et al. Platelet TGF-beta1 contributions to plasma TGF-beta1, cardiac fibrosis, and systolic dysfunction in a mouse model of pressure overload. Blood. 2012; 119(4):1064–74. DOI: 10.1182/blood-2011-09-377648 [PubMed: 22134166]
8. Assoian RK, Komoriya A, Meyers CA, Miller DM, Sporn MB. Transforming growth factor-beta in human platelets. Identification of a major storage site, purification, and characterization. JBiolChem. 1983; 258(11):7155–60.
9. Haemmerle M, Bottsford-Miller J, Pradeep S, Taylor ML, Choi HJ, Hansen JM, et al. FAK regulates platelet extravasation and tumor growth after antiangiogenic therapy withdrawal. JClinInvest. 2016; 126(5):1885–96.
10. Kerbel RS. Tumor angiogenesis. The New England journal of medicine. 2008; 358(19):2039–49. DOI: 10.1056/NEJMra0706596 [PubMed: 18463380]
11. Goumans MJ, Liu Z, ten Dijke P. TGF-beta signaling in vascular biology and dysfunction. Cell research. 2009; 19(1):116–27. DOI: 10.1038/cr.2008.326 [PubMed: 19114994]
12. Pepper MS. Transforming growth factor-beta: vasculogenesis, angiogenesis, and vessel wall integrity. Cytokine & growth factor reviews. 1997; 8(1):21–43. [PubMed: 9174661]
13. Sabrkhany S, Griffioen AW, Oude Egbrink MG. The role of blood platelets in tumor angiogenesis. Biochimica et biophysica acta. 2011; 1815(2):189–96. DOI: 10.1016/j.bbcan.2010.12.001 [PubMed: 21167916]
14. Verheul HM, Hoekman K, Lupu F, Broxterman HJ, van der Valk P, Kakkar AK, et al. Platelet and coagulation activation with vascular endothelial growth factor generation in soft tissue sarcomas. Clinical cancer research : an official journal of the American Association for Cancer Research. 2000; 6(1):166–71. [PubMed: 10656446]
15. Roby KF, Taylor CC, Sweetwood JP, Cheng Y, Pace JL, Tawfik O, et al. Development of a syngeneic mouse model for events related to ovarian cancer. Carcinogenesis. 2000; 21(4):585–91. [PubMed: 10753190]

16. Cho MS, Vasquez HG, Rupaimoole R, Pradeep S, Wu S, Zand B, et al. Autocrine effects of tumor-derived complement. Cell Rep. 2014; 6(6):1085–95. [PubMed: 24613353]
17. Hu Q, Cho MS, Thiagarajan P, Aung FM, Sood AK, Afshar-Kharghan V. A small amount of cyclooxygenase 2 (COX2) is constitutively expressed in platelets. Platelets. 2016; :1–4. DOI: 10.1080/09537104.2016.1203406
18. Hu Q, Gao F, Tian W, Ruteshouser EC, Wang Y, Lazar A, et al. Wt1 ablation and Igf2 upregulation in mice result in Wilms tumors with elevated ERK1/2 phosphorylation. The Journal of clinical investigation. 2011; 121(1):174–83. DOI: 10.1172/jci43772 [PubMed: 21123950]
19. Borsig L. The role of platelet activation in tumor metastasis. Expert review of anticancer therapy. 2008; 8(8):1247–55. DOI: 10.1586/14737140.8.8.1247 [PubMed: 18699763]
20. Akhurst RJ, Derynck R. TGF-beta signaling in cancer--a double-edged sword. Trends in cell biology. 2001; 11(11):S44–51. [PubMed: 11684442]
21. Drabsch Y, ten Dijke P. TGF-beta signalling and its role in cancer progression and metastasis. Cancer metastasis reviews. 2012; 31(3–4):553–68. DOI: 10.1007/s10555-012-9375-7 [PubMed: 22714591]
22. Papageorgis P, Stylianopoulos T. Role of TGFbeta in regulation of the tumor microenvironment and drug delivery (review). International journal of oncology. 2015; 46(3):933–43. DOI: 10.3892/ijo.2015.2816 [PubMed: 25573346]
23. Martins VL, Caley MP, Moore K, Szentpetery Z, Marsh ST, Murrell DF, et al. Suppression of TGFbeta and Angiogenesis by Type VII Collagen in Cutaneous SCC. Journal of the National Cancer Institute. 2016; 108(1)doi: 10.1093/jnci/djv293
24. Neuzillet C, Tijeras-Raballand A, Cohen R, Cros J, Faivre S, Raymond E, et al. Targeting the TGFbeta pathway for cancer therapy. Pharmacology & therapeutics. 2015; 147:22–31. DOI: 10.1016/j.pharmthera.2014.11.001 [PubMed: 25444759]
25. Roy LO, Poirier MB, Fortin D. Transforming growth factor-beta and its implication in the malignancy of gliomas. Targeted oncology. 2015; 10(1):1–14. DOI: 10.1007/s11523-014-0308-y [PubMed: 24590691]
26. Sanchez-Elsner T, Botella LM, Velasco B, Corbi A, Attisano L, Bernabeu C. Synergistic cooperation between hypoxia and transforming growth factor-beta pathways on human vascular endothelial growth factor gene expression. J Biol Chem. 2001; 276(42):38527–35. DOI: 10.1074/jbc.M104536200 [PubMed: 11486006]
27. Liao S, Liu J, Lin P, Shi T, Jain RK, Xu L. TGF-beta blockade controls ascites by preventing abnormalization of lymphatic vessels in orthotopic human ovarian carcinoma models. Clinical cancer research : an official journal of the American Association for Cancer Research. 2011; 17(6):1415–24. DOI: 10.1158/1078-0432.ccr-10-2429 [PubMed: 21278244]
28. Dunfield LD, Nachtigal MW. Inhibition of the antiproliferative effect of TGFbeta by EGF in primary human ovarian cancer cells. Oncogene. 2003; 22(30):4745–51. DOI: 10.1038/sj.onc.1206617 [PubMed: 12879019]
29. Jakowlew SB. Transforming growth factor-beta in cancer and metastasis. Cancer metastasis reviews. 2006; 25(3):435–57. DOI: 10.1007/s10555-006-9006-2 [PubMed: 16951986]
30. Gatza CE, Oh SY, Blobe GC. Roles for the type III TGF-beta receptor in human cancer. Cellular signalling. 2010; 22(8):1163–74. DOI: 10.1016/j.cellsig.2010.01.016 [PubMed: 20153821]
31. Gharwan H, Bunch KP, Annunziata CM. The role of reproductive hormones in epithelial ovarian carcinogenesis. Endocrine-related cancer. 2015; 22(6):R339–63. DOI: 10.1530/erc-14-0550 [PubMed: 26373571]
32. Hempel N, How T, Dong M, Murphy SK, Fields TA, Blobe GC. Loss of betaglycan expression in ovarian cancer: role in motility and invasion. Cancer Res. 2007; 67(11):5231–8. DOI: 10.1158/0008-5472.can-07-0035 [PubMed: 17522389]
33. Connolly EC, Freimuth J, Akhurst RJ. Complexities of TGF-beta targeted cancer therapy. International journal of biological sciences. 2012; 8(7):964–78. DOI: 10.7150/ijbs.4564 [PubMed: 22811618]
34. Massague J. TGFbeta in Cancer. Cell. 2008; 134(2):215–30. DOI: 10.1016/j.cell.2008.07.001 [PubMed: 18662538]

35. Akhurst RJ, Hata A. Targeting the TGFbeta signalling pathway in disease. Nature reviews Drug discovery. 2012; 11(10):790–811. DOI: 10.1038/nrd3810 [PubMed: 23000686]

36. Connolly EC, Saunier EF, Quigley D, Luu MT, De Sapio A, Hann B, et al. Outgrowth of drug-resistant carcinomas expressing markers of tumor aggression after long-term TbetaRI/II kinase inhibition with LY2109761. Cancer Res. 2011; 71(6):2339–49. DOI: 10.1158/0008-5472.can-10-2941 [PubMed: 21282335]

Translational Relevance

Our studies showed that Tgfβ1 released from platelets increases proliferation rate of cancer cells and neoangiogenesis in the tumor, and promotes the growth of ovarian cancer. Anti-platelet reagents by preventing activation and degranulation of platelets, and hence by decreasing Tgfβ1 released from platelets may have therapeutic benefits in ovarian cancer. Inhibitors of the Tgfβ receptor (TgfβR) complex reduce the pro-growth effects of platelets on ovarian cancer and diminish tumor growth. The therapeutic benefit of TgfβR inhibitors is more pronounced if initiated earlier during the course of cancer treatment. Our results raise the possibility of a clinical benefit for using anti-platelet reagents in conjugation to surgery and chemotherapy in patients with ovarian cancer. Furthermore, in patients with ovarian cancer and thrombocytosis, the addition of TgfβR inhibitors to the other therapeutic modalities may enhance the response rate.

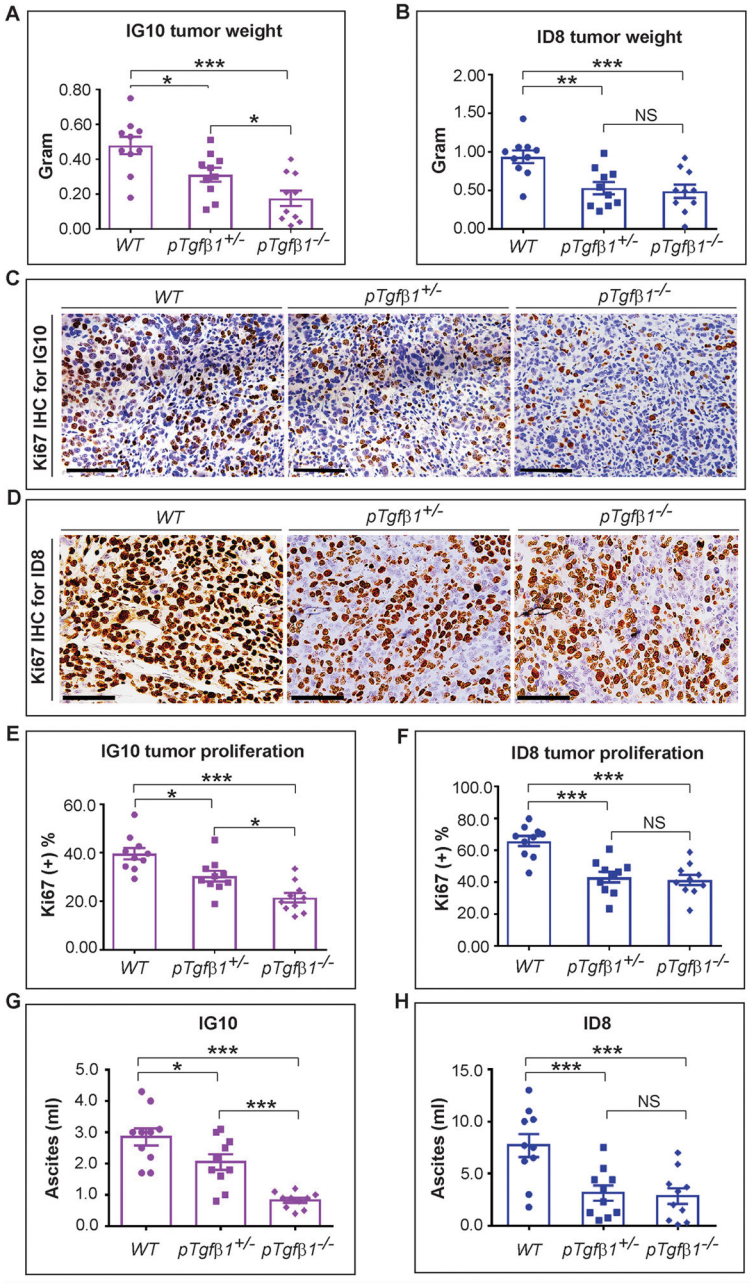

Figure 1.

Platelet Tgfβ1 and growth of orthotopic murine ovarian cancer. 8–10 weeks after i.p. injection of murine ovarian cancer cells (IG10 and ID8) tumor nodules were resected from moribund mice. (A) Aggregate weight of IG10-induced tumor nodules in 3 groups of mice (n=10/group): WT, *pTgfβ1*$^{+|-}$, *and pTgfβ1*$^{-|-}$. (B) Aggregate weight of ID8-induced tumor nodules in 3 groups of mice (n=10/group): WT, *pTgfβ1*$^{+|-}$, *and pTgfβ1*$^{-|-}$. (C) Representation of Ki67 immunostaining of sections of IG10-induced tumor nodules. (D) Representation of Ki67 immunostaining of sections of ID8-induced tumor nodules. Scale bars in panels C & D are 200 μm. (E) Quantification of Ki67 positivity (proliferation index)

in IG10-induced tumors (n=10). (F) Quantification of Ki67 positivity (proliferation index) in ID8-induced tumors (n=10). Ascites volume associated with (G) IG10 and (H) ID8 cell-induced tumors in WT, $pTgf\beta1^{+1-}$, *and* $pTgf\beta1^{-1-}$ mice (n=10 mice/group).

The ANOVA analysis was performed on the experimental results represented in A–H. The corresponding p values of the F-test were 0.002 (A), 0.001 (B), 0.00001 (E), 0.00001 (F), <0.00001 (G), and 0.007 (H). Student's t-test was carried out for statistical analysis, and significance levels were as follows: $p < 0.05$ for *, $p < 0.01$ for **, $p < 0.001$ for ***. Averaged data are presented as the mean ± SEM.

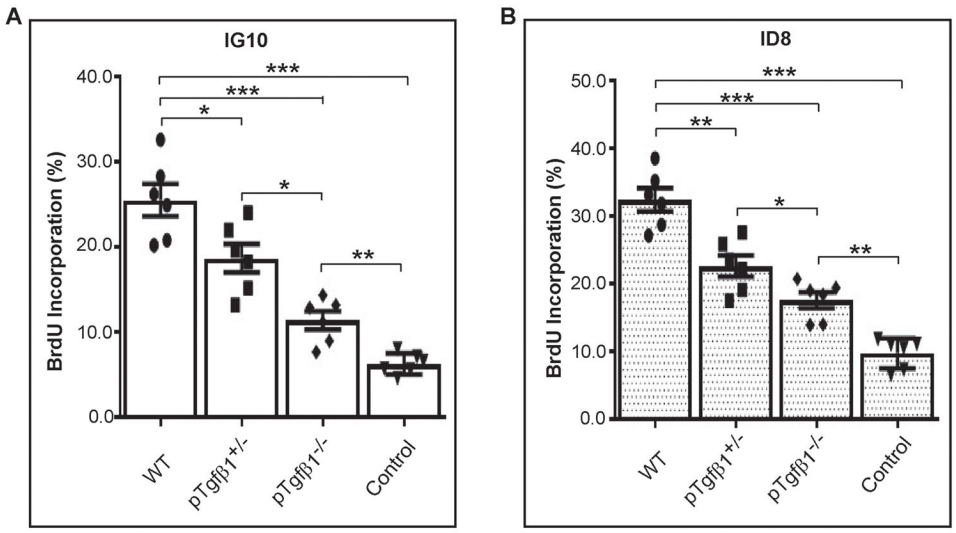

Figure 2.

Effect of platelet Tgfβ1 on cancer cell proliferation *in vitro*. Fresh platelets isolated from whole blood of mice were coincubated with murine ovarian cancer cells (IG10 and ID8) and the cell proliferation rate was measured by quantifying BrdU incorporations (A) Proliferation rate of IG10 cells coincubated with platelets isolated from WT, $pTgf\beta1^{+|-}$, *or* $pTgf\beta1^{-|-}$ mice. IG10 cells incubated in buffer were used as controls. (B) Proliferation rate of ID8 cells coincubated with platelets from WT, $pTgf\beta1^{+|-}$, *or* $pTgf\beta1^{-|-}$ mice. ID8 cells incubated in buffer were used as controls. n=3 mice per each genotype and each assay was performed in duplicate. The ANOVA analysis was performed on the results of both experiments. The corresponding p values of the F-test were 0.00006 (A), and < 0.00001 (B). Student's t-test is carried out for statistical analysis and significance levels indicated are as follows: $p < 0.05$ for *, $p < 0.01$ for **, $p < 0.001$ for ***. Averaged data are presented as the mean ± SEM.

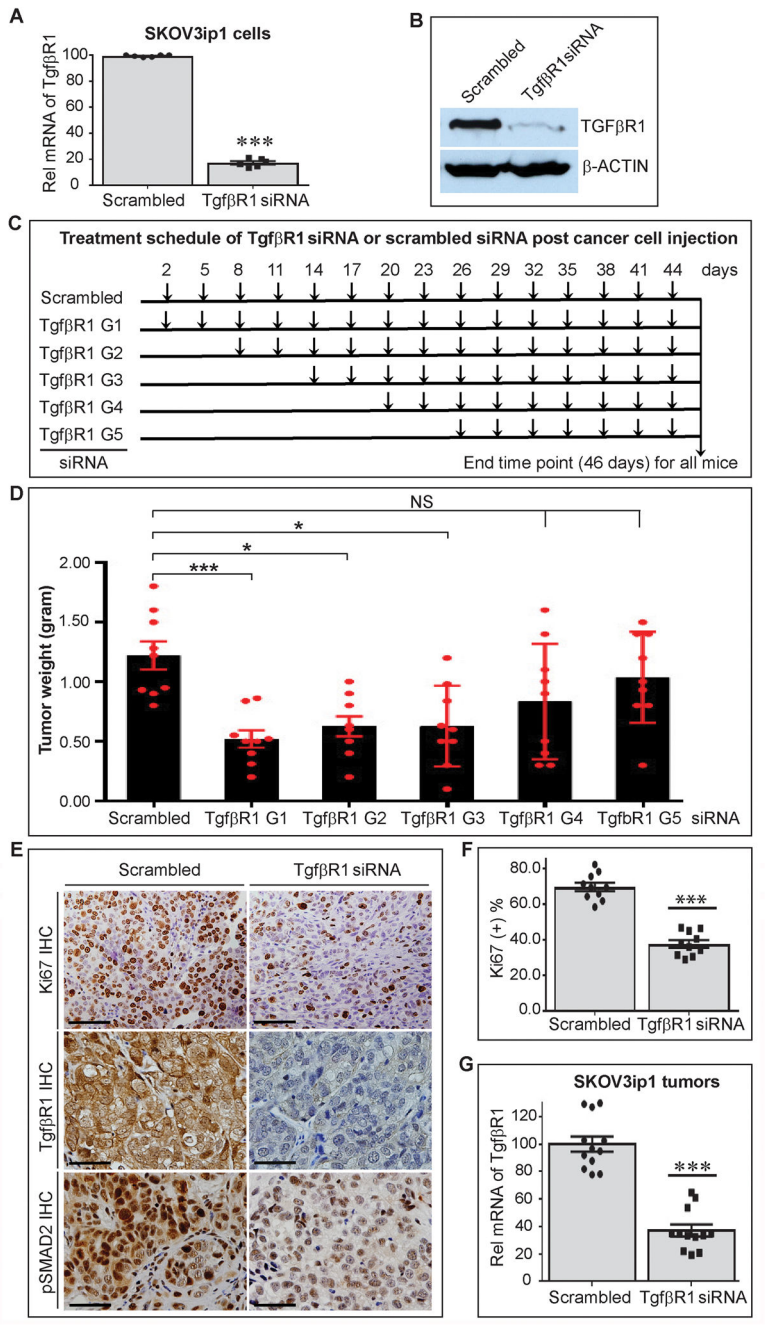

Figure 3.

Expression of TgfβR1 on ovarian cancer and growth of orthotopic tumors in mice. Expression of TgfβR1 on human ovarian cancer cells (SKOV3ip1) after injection to mice was reduced using human (h) TgfβR1 siRNA at different time points, and final growth of orthotopic tumors was compared between different groups. (A) Quantification of TgfβR1 mRNA level in SKOV3ip1 cells incubated with scrambled siRNA or hTgfβR1 siRNA *in vitro* for 48 hours by qRT-PCR (n=6). (B) Effect of hTgfβR1 siRNA and scrambled siRNA on the expression of TgfβR1 at the protein level in SKOV3ip1 cells. A representative

Western-blot is shown (n=3). (C) Experimental design for reducing expression of TgfβR1 on SKOV3ip1 cells in tumor-bearing nude mice at different time points using *in vivo* delivery of hTgfβR1 siRNA by DOPC-based liposomes. Each experimental group (n=9 mice/group) received i.p. injection of hTgfβR1 siRNA every 3 days, starting at day 2(G1), day 8 (G2), day 14 (G3), day 20 (G4), or day 26 (G5) after injection of cancer cells that continued until day 46. Tumor-bearing mice in control group (scrambled) received i.p. injection of scrambled siRNA every 3 days starting on day 2 until day 46. (D) Aggregate weight of SKOV3ip1-induced tumor nodules in different treatment and control groups. (E) Representation of Ki67, TgfβR1, and phosphorylated SMAD2 (pSMAD2) immunostaining of sections of SKOV3ip1-induced tumor nodules. Scale bars are 100 μm. (F) Quantification of Ki67 positivity (proliferation index) in SKOV3ip1-induced tumors (n=10, 5 mice per group, 1 nodule from each mouse, and 2 sections per nodule). Scale bars are 200 μm. (G) Quantification of TgfβR1 mRNA level in SKOV3ip1-induced tumors resected from mice treated with scrambled siRNA or hTgfβR1 siRNA. The ANOVA analysis was performed on the results in D and the p value was <0.00001. Student's t-test was carried out for statistical analysis, and significance levels were as follows: $p < 0.05$ for *, $p < 0.01$ for **, $p < 0.001$ for ***. NS: no significance. Averaged data are presented as the mean ± SEM.

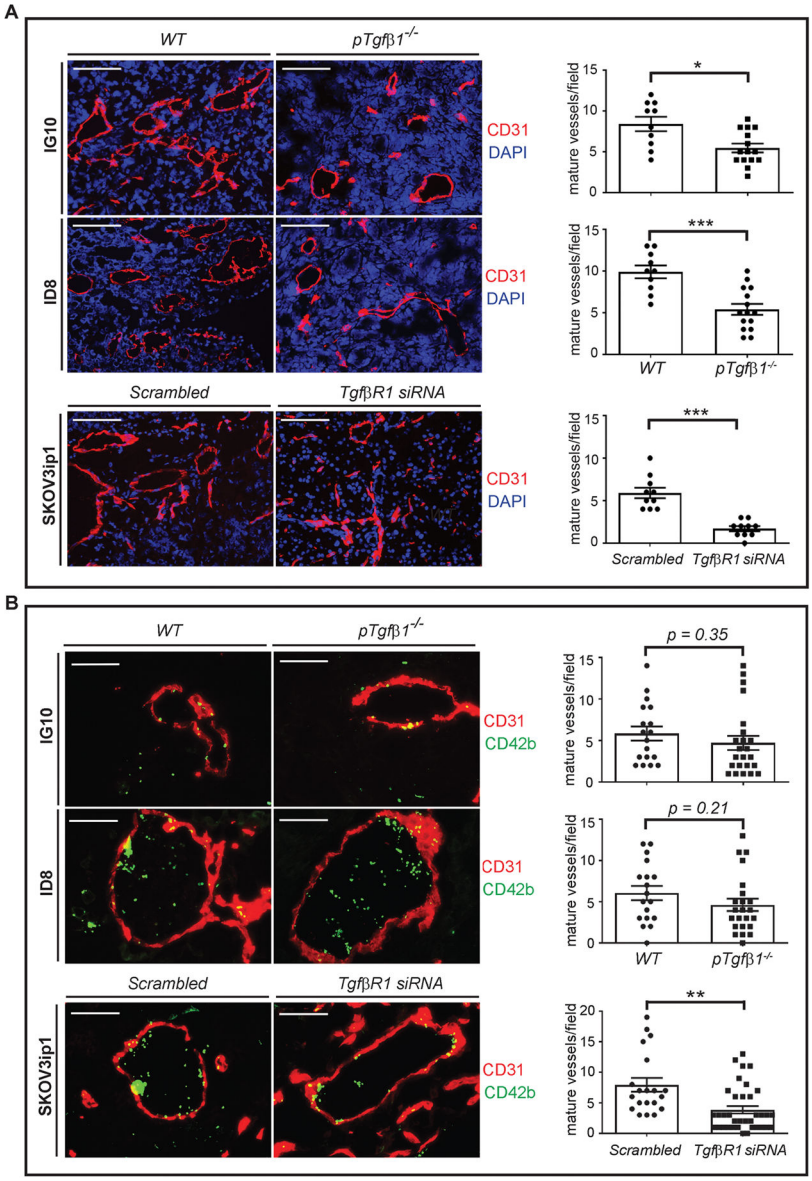

Figure 4.

Effect of platelet's Tgfβ1 and ovarian cancer cell's TgfβR1 on neoangiogenesis and platelet extravasation. Sections of IG10, ID8, and SKOV3ip-induced tumor nodules were stained with DAPI (nuclei of cancer cells), CD31 (endothelial cells) and CD42b (platelets) and analyzed by immunofluorescence microscopy. (A) The left side panel shows representative of micrographs from sections of tumor nodules. Blood vessels were detected by lumens encircled with CD31+ cells. The right side panel shows quantification of blood vessel density in each group of mice (5 mice/group, at least 3 tumor nodules per mouse, 1 section per nodule, and 2 or more HPF per section). Scale bars are 200 μm. (B) The left side panel shows representative micrographs of sections of tumor nodules. Extravasated platelets were detected by intratumor and extravascular CD42b+ cells. The right side panel shows quantification of extravasated platelets in each group of mice (5 mice/group and at least 3

tumor nodules per mouse, 2 random sections per nodule and 2 or more HPF per section). Scale bars are 100 μm. Student's t-test is carried out for statistical analysis and significance levels indicated are as follows: $p < 0.05$ for *, $p < 0.001$ for ***. Averaged data are presented as the mean ± SEM.